

# Uptake and translocation of nanoplastics in mono and dicot vegetables

Eric Zytowski<sup>1,2</sup>  | Mohanna Mollavali<sup>1</sup> | Susanne Baldermann<sup>1,3</sup> 

<sup>1</sup>Leibniz Institute for Vegetable and Ornamental Crops (IGZ), Grossbeeren, Germany

<sup>2</sup>Institute of Nutritional Science, University Potsdam, Nuthetal, Germany

<sup>3</sup>Faculty for Life Sciences: Food, Nutrition and Health, Campus in Kulmbach University of Bayreuth, Bayreuth, Germany

## Correspondence

Susanne Baldermann, Faculty for Life Sciences: Food, Nutrition and Health, Campus in Kulmbach University of Bayreuth, Bayreuth, Germany.

Email: [Susanne.Baldermann@uni-bayreuth.de](mailto:Susanne.Baldermann@uni-bayreuth.de)

## Funding information

EFRE funds, Grant/Award Number: 85037644

## Abstract

The excessive production and use of plastics increase the release of micro- and nanoplastics (MNPs) into the environment. In recent years, research has focused on the occurrence of MNPs in air, soil and water. Nevertheless, there is still a lack of knowledge regarding MNPs in plants. To determine the load, translocation of MNPs and their effects on metabolism, pak choi, tomato, radish and asparagus have been exposed with fluorescent-labelled poly(methyl methacrylate) or polystyrene (PS) MNPs. The entry of nanoparticles (NPs) of various sizes (100–500 nm) and surface modifications (unmodified, COOH or NH<sub>2</sub>) into plants has been demonstrated using confocal laser scanning microscopy (CLSM). The translocalization from root to shoot and the accumulation of NP in the intercellular spaces were regardless of the surface modification. In addition, metabolomics was used to evaluate metabolic changes induced by MNPs in pak choi. Changes in phenolic compounds, phytohormone derivatives and other classes of compounds known to be triggered by various environmental stresses have been identified. The present study demonstrates the uptake and translocalization of MNPs in edible parts of vegetables and may pose a hazard for humans.

## KEYWORDS

CLSM, LC/Q-TOF, metabolomics, micro- and nanoplastics

## 1 | INTRODUCTION

The production and use of plastics is increasing worldwide, and there is growing global concern about the risk of plastic pollution (UN Environment Programme, 2022). Toxic substances released from plastic's degradation can cause ambient air, soil and water pollution (Lwanga et al., 2022). In 2021, 57.2 million metric tons were produced in Europe and 390.7 million metric tons of plastic in the world, of which around 4% are used in agriculture (Plastics Europe, 2022). Due to degradation of plastics e.g. from plastic mulch films or input

through compost and sewage, micro- and nanoplastics (MNPs) can accumulate in soil and contaminate agricultural land (Yu et al., 2022).

Nanoplastic particles (NP) are 1–1000 nm, whereas microplastic particles (MP) have sizes of 1–1000 µm (Hartmann et al., 2019). There are two groups of MNPs in the environment; primary; which is released from some industrial products such as cosmetics, detergents, tires and industrial abrasives and secondary; which is generated from degradation and fragmentation of larger plastic materials for instance due to mechanical or environmental influences, for example, tillage or UV radiation (Duis & Coors, 2016).

Eric Zytowski and Mohanna Mollavali are Joint first author.

This is an open access article under the terms of the [Creative Commons Attribution-NonCommercial-NoDerivs](https://creativecommons.org/licenses/by-nc-nd/4.0/) License, which permits use and distribution in any medium, provided the original work is properly cited, the use is non-commercial and no modifications or adaptations are made.

© 2024 The Author(s). *Plant, Cell & Environment* published by John Wiley & Sons Ltd.

Over the last decade, several studies have evaluated the toxicity of NP in aquatic ecosystems (Gaylarde et al., 2021; Koelmans et al., 2015). For instance, altered behaviour of fishes receiving polystyrene (PS) NP through the food chain was demonstrated (Mattsson et al., 2015). They reported that fishes fed with NP had altered hunting behaviour and lower activity as a result of their cellular function disturbance and metabolomic changes caused by PS particles.

MNPs in agriculture can originate from direct sources, such as mulch films (polyethylene [PE], polypropylene [PP], polylactic acid), greenhouse materials (multi-layered PE, PP, polyvinylchloride films), and soil conditioners (polyurethane foam and PS flakes). These particles can also come from indirect sources, such as the use of compost (Vithanage et al., 2021), treated wastewater, and sewage sludge (Qi et al., 2020). Recently, it was shown for the first time that plants can uptake and accumulate NP, depending on plant species, particle size, concentration and availability, time of exposure and their surface charge/modification (Spielman-Sun et al., 2019; Sun et al., 2020; Yu et al., 2021). This is an unexplored route for MNPs to enter the food chain and potentially pose a risk to human health. Nonetheless, there is scarce information available on the entry and translocation of MNPs in vegetables, specifically the edible parts. Furthermore, there is a lack of methodologies for the detection of MNPs in plant's organs and an existing knowledge gap in identifying metabolic changes in plants affected by MNPs (Dong et al., 2021; Lian et al., 2022; Liu et al., 2022; Sun et al., 2020). Therefore, extensive studies on the impact of different MNPs on different vegetable crops have to be performed. Unmodified PS MNPs penetrated carrot plants in a hydroponic system and impaired their quality (Dong et al., 2021). In a separate study, it was observed that PS MNPs accumulated in the root system of cucumber plants and were subsequently translocated to all aboveground tissues. This resulted in a notable impact on the quality of the fruit. (Li, Li, et al., 2021). Furthermore, it was estimated that between 13 and 18% of the uptaken PS MNPs were translocated to the aerial parts of garden cress (Sahai et al., 2024). The inhibition of lignin and jasmonate biosynthesis in rice plants treated with PS NP has been reported (Zhou et al., 2021). PS MNPs triggered oxidative stress in rice plants in a hydroponic system and caused changes in the amino acid metabolic pathway and also changed the root architecture. Interestingly, these changes were size dependent, as 1  $\mu\text{m}$  PS showed stronger phytotoxicity than 100 nm (Wu et al., 2021). The particle size also had an impact on plant growth. A positive effect was demonstrated at low PS MNPs concentrations, while higher concentrations had a negative impact (hormesis) in tobacco and oilseed rape (Rong et al., 2024; Tian et al., 2024). In a first quantitative study the existence of varying concentrations of polymers in a number of crops, including field-grown cowpea, flowering cabbage, rutabagas and chieh-qua was demonstrated (Ye et al., 2024).

PS MNPs have become a model for toxicological research as they are one of the five most commonly produced plastics worldwide, commercially available as fluorescently labelled particles, easy to synthesise and process into NP (Andrady & Neal, 2009;

Kokalj et al., 2021; Liu et al., 2024). Poly(methyl methacrylate) (PMMA) is a versatile synthetic polymer known as acrylic and also commonly used in NP studies (Li, Gao, et al., 2021). A significant impact of NP characteristics and plant species on particles entry and distribution in different organs has been demonstrated (Spielman-Sun et al., 2019). In this model study with  $\text{CeO}_2$ -nanoparticles (NPs), positively charged NPs had higher uptake by roots, whereas, negatively charged particles were more efficiently translocated. The different root architecture between dicots and monocots must be taken into account. Dicots have only one primary root and several orders of lateral roots whereas monocot roots are fibrous and form additional axial roots that emerge from the stem (Koevoets et al., 2016). Recently, it was also confirmed that plants can uptake and translocate NP via leaf stomata (Lian et al., 2021; Sun et al., 2020).

Before more advanced research can be conducted on how MNPs affect plant growth and molecular and metabolic pathways, understanding the factors affecting on the uptake accumulation and translocation of MNPs in different plants is essential. There are numerous methodologies available for the detection of MNPs in plants, including pyrolysis gas chromatography coupled with mass spectrometry (Py-GC/MS), confocal laser scanning microscopy (CLSM), scanning electron microscopy (SEM), micro Fourier transform infrared spectrometry ( $\mu$ -FTIR), and micro Raman spectrometry. Alternatively, inductively coupled plasma spectrometry can be employed for the detection of metal-doped plastic particles, such as those containing europium (Eu) or palladium (Pd) (Hua et al., 2023; Li, Gao, et al., 2021; Luo et al., 2022). In this study, to investigate the factors affecting the absorption, accumulation and translocation of MNPs in different vegetables, a series of consistent and comparative experiments using our optimised CLSM detection method with fluorescent MNPs of varying types, sizes and surface modifications in mono- and dicot plants have been conducted. PS and PMMA have been selected to illustrate if the chemical properties of MNPs play a role in plant's uptake and translocation. To evaluate the role of various entry routes of MNPs; we considered particles entry from soil, from liquid nutrient solution and foliar uptake. We hypothesised that: (1) Systematic differences between mono and dicots root type provides different root surface area and affects the soil volume availability which in consequence can cause altered uptake and relocation of MNPs in various plant species. (2) MNPs can act as abiotic stress and inhibit plant's growth and affect metabolism. Therefore, the quality of plant-based food will be negatively affected.

Taken together, the study provides an optimised detection method for screening single particles of MNPs in plants and highlights the need of further metabolomics analysis for qualification of MNPs impact on plant's secondary metabolites in future research in this critical field. Our findings on the uptake and accumulation of MNPs in plants can help not only to assess NP as potential transporters for plant research, but also to utilise them for future concepts in plant protection. Furthermore, our research can also help decision-makers on developing new regulations on environmental protection and the use of MNPs.

## 2 | MATERIAL AND METHODS

### 2.1 | Plant material

Seeds of pak choi (*Brassica rapa subsp. chinensis* cv. Black Behi), tomato (*Solanum lycopersicum* cv. MoneyMaker, Micro Tom), radish (*Raphanus sativus* cv. Solaris) as dicots and asparagus (*Asparagus officinalis* cv. Avalim) as monocot, have been used for our experiments. For the model uptake experiments, seeds were surface sterilised with 0.1% TWEEN®20 for 20 min, with 95% ethanol for 1 min, followed by incubation for 5 min in 5.25% hypochlorite solution and finally washed five times with sterilised deionized water. To simulate different ways of uptake, pak choi seeds then placed on ½ Murashige-Skoog (MS, Plant agar, Duchefa, pH 4.2) medium with agar, on PE nets in contact with ½ MS solution or on soil in sterile boxes (Sterivent High Container, Duchefa, 107 × 94 × 96 mm). To prevent any contamination in boxes with ½ MS medium with agar, 0.05% PPM (Plant Preservative Mixture, Plant Cell Technology) has been added. The soil (Einheitserde type P, pH 5.8, Germany) was sterilised and oven dried before use (20 min at 121°C and then dried at 55°C for 48 h in oven). After placing the seeds, the boxes were then kept at 4°C for 48 h then transferred to the growth chamber (CONVIRON A 1000) with controlled conditions (16 h photoperiod with 80 µmol/m<sup>2</sup>s light intensity at 22°C light/18°C dark cycle). To verify our detection method we have sown tomato, radish and asparagus in ½ MS medium following the same procedure except that asparagus seeds have been kept in incubator at 25°C and darkness until germination. Pictures of the experimental setups are shown in Supporting Information Material S1: Figure S1.

### 2.2 | Properties of plastic particles used in this study

Fluorescence-labelled PMMA NP with a nominal size of 401–450 nm and PS NP with nominal sizes of 100 and 500 nm were used. The actual sizes of the particles were measured to be 430 ± 23 nm (PMMA 401–450 nm), 131 ± 50 nm (PS-COOH 100 nm), 94 ± 20 nm (PS-NH<sub>2</sub> 100 nm), 122 ± 26 nm (PS plain 100 nm), 563 ± 91 nm (PS-COOH 500 nm) and 590 ± 69 nm (PS-NH<sub>2</sub> 500 nm). The PMMA NP surface is carboxylated (COOH) and has a zeta potential of -40 mV. The PS NP have different surface modifications with different zeta potentials: PS 100 nm unmodified (plain, -52 mV), carboxylated (COOH, -60 mV) and amino groups (NH<sub>2</sub>, -34 mV (isoelectric point = pH 3.3)) and PS 500 nm carboxylated (COOH, -58 mV) and amino groups (NH<sub>2</sub>, -49 mV (isoelectric point = pH 4.5)). The PS-NH<sub>2</sub> are amphoteric particles, at pH=4.2 (½ MS medium) the 500 nm particles are positively charged. The size distribution of the PS particles and the zeta potential was measured by micromod in deionized water with a Zetasizer NanoZS90 (MALVERN Instruments Ltd.), for the PMMA particles the data was obtained from the certificate of analysis for the used particle batch (PolyAn, REF: 20702425, LOT: PFA201104K). The primary particle material (PMMA, PS) was confirmed by specific markers (PMMA: methyl methacrylate,

PS: styrene monomer, dimer, trimer) by means of TED-GC/MS as described in the literature (Braun et al., 2020; Duemichen et al., 2019). The fluorescent dyes are embedded directly into the MNPs for a homogeneous distribution of the dye and reduction of leaching (product description PolyAn). The stability of the fluorescence dye of the PMMA particles was analysed with an Infinite M200 Pro plate reader (Tecan Group, Ltd.). After 5 days, the fluorescence intensity of the PMMA particles decreased by 34.6 ± 9% at pH 4.8, 8.8 ± 1.6% at pH 5.8, 7.1 ± 3.5% at pH 6.8, and 4.6 ± 4.7% at pH 7.8 (Supporting Information Material S1: Figure S2). Before use, the particles have been suspended by vortexing for 1 min and ultrasonication for 5 min.

A summary with the specific characteristics of the MNPs is given in the Supporting Information Material S1: Table S1.

### 2.3 | Application of micro and nanoplastics

#### 2.3.1 | Uptake of NP from agar medium, solution, soil and after foliar application

To accomplish our goal, a model experiment with 6 well plates and different matrixes have been designed (Supporting Information Material S1: Figure S1). Two wells have been filled either with 5 mL ½ MS medium, 5 mL ½ MS solution or 3 g of soil. Two sterilised pak choi seeds have been placed in each well and the plates then have been kept in growth chambers under control condition (16 h photoperiod at 22°C light with 80 µmol/m<sup>2</sup>s light intensity and 18°C at dark cycle). To avoid root hypoxia in our ½ MS solution wells, seeds have been placed on a sterilised PE net with two holes in a way that the roots were in touch with the liquid medium. After 3 weeks of germination, the plants were treated with NP solution as described below and harvested 4 days later.

The ½ MS medium was supplemented with 160 µL of diluted NP solution containing PMMA particles with a concentration of 1.25 mg/mL for 401–450 nm particles and 0.625 mg/mL for 2 µm particles (corresponding to 0.2 mg or 0.1 mg/treatment, respectively). Additionally, 10 µL of undiluted NP solution with a concentration of 10 mg/mL for 401–450 nm particles and 5 mg/mL for 2 µm particles was added to the ½ MS solution (corresponding to 0.1 mg or 0.05 mg/treatment, respectively). The concentration of NP solution for soil was the same as that for the ½ MS medium. To investigate the influence of particle size and surface modification on the uptake in pak choi, carboxyl-modified (PS-COOH), amino-modified (PS-NH<sub>2</sub>) or plain (neutral coating, PS-plain) PS particles of different sizes (100 and 500 nm) were used. The ½ MS medium was supplemented with 80 µL of diluted NP solution containing PS particles with a concentration of 1.250 mg/mL for 100 nm particles and 3.125 mg/mL for 500 nm particles (corresponding to 0.1 mg or 0.25 mg/treatment, respectively). The reduction in concentration observed in the ½ MS medium/solution and soil following initial administration did not undergo further investigation. Although the experimental setups differ (solid ½ MS medium vs. hydroponic experiment), the initial concentrations added in our experiment are comparable to those reported in the literature (Li, Luo, Peijnenburg, et al., 2020; Luo, Li et al., 2020).

Plants for foliar uptake were grown on wells on 5 mL  $\frac{1}{2}$  MS medium, without adding labelled NP to the medium. Three weeks after germination, NP were applied on seedlings by adding a 4  $\mu$ L droplet (1  $\mu$ L NP with 3  $\mu$ L  $\frac{1}{2}$  MS solution (PMMA 401–450 nm:  $c_{\text{particles}} = 2.5$  mg/mL (0.01 mg/treatment), PMMA 2  $\mu$ m:  $c_{\text{particles}} = 1.25$  mg/mL (0.005 mg/treatment) onto the adaxial surface of the leaf. Control plants were exposed to 4  $\mu$ L of  $\frac{1}{2}$  MS solution. After 10 days, leaves have been collected and the surfaces intensively washed with distilled water before slide preparation. The experiment was carried out in independent triplicates.

### 2.3.2 | Imaging by CLSM

For the detection of labelled MNPs a CLSM was used. Microscopic imaging was performed on an Axioplan 2 Imaging Microscope (Carl Zeiss) equipped with an LSM 510 META (Carl Zeiss) laser scanning module and an objective LD LCI Plan-Apochromat 25x/0.8 ImmCorr DIC M27. Images were acquired with an AxioCam (Carl Zeiss, Germany, Jena) and processed with ZEN 3.2 (blue edition) software. Labelled MNPs fluorescence was excited with an Argon laser at  $\lambda = 488$  nm and emission was detected from  $\lambda = 505$ –530 nm with a band-pass filter ( $\lambda = 505$ –530 nm), where the fluorescence of the PMMA particles is shown in red and from the PS particles in purple (Supporting Information S1: Table S1). Auto fluorescence was detected at  $\lambda \geq 505$  nm using a low-pass filter, and the resulting fluorescence is green in colour. Signal intensity of auto fluorescence was adjusted with excitation laser intensity to control samples. Fresh hand-cut sections from the root tip, maturation region, stem (longitudinal and transverse sections), and leaf (upper epidermis and transverse section of midrib) were prepared using a sharp stirrup-shaped blade (Carl Roth, type 210) after washing the leaves (foliar uptake experiment) and roots with distilled water. The use of hand cutting was preferred to freeze sectioning due to the ease with which the blades can be cleaned after each cut, thus reducing the risk of cross-contamination. The specimens then have been placed on glass slides (Eprelia frosted microscope slides, ground 90°) and covered with a few drops of 50% corn syrup/water and a coverslip (Carl Roth, 24  $\times$  50 mm) to keep the samples hydrated.

### 2.3.3 | Uptake from agar medium and metabolomic profiling

To investigate the impact of MNPs on plant's metabolite profiles and growth parameters, nine sterilised pak choi seeds have been germinated on  $\frac{1}{2}$  MS medium in sterile boxes in triplicates (six boxes in total). Four weeks after germination, 80  $\mu$ L (corresponding to 0.1 mg/treatment, respectively) of MNPs solution (PMMA 401–450 nm:  $c_{\text{particles}} = 1.25$  mg/mL) was pipetted around the roots of each plant and the plants were harvested after 4 days. The fresh weight of the roots and shoots was determined before freezing the samples in liquid nitrogen. Control plants were grown and kept under equal conditions until harvest.

## 2.4 | Nontargeted analysis of metabolomics profiling

A modified nontargeted analysis (Errard et al., 2015), by Agilent 6546 LC/Q-TOF coupled with an Agilent 1290 Infinity UHPLC equipped with an electrospray ionisation source in positive and negative ionisation mode has been employed to evaluate differences in the metabolic profiling of pak choi roots and shoots with or without NP application. Plant material from freeze dried roots and shoots of pak choi plants have been pulverised with a Retsch ball mill to a fine powder. Ten milligrams of grounded material were extracted with 200  $\mu$ L of 70% methanol (MeOH) acidified with 0.1% formic acid. The samples then sonicated on ice for 10 min and centrifuged at 3500 rpm for 5 min. The extract was filtered through 0.2  $\mu$ m polytetrafluoroethylene membrane. The separation of 1  $\mu$ L sample was performed using an Agilent Zorbax Extend–C18 Rapid resolution HT (50  $\times$  2.1 mm, 1, 1.8  $\mu$ m) column. The temperatures of the auto-sampler and the column oven were set to 19°C and 30°C, respectively. Two mobile phases (A: 0.01% formic acid in ultrapure water and B: 0.01% formic acid in acetonitrile) have been applied with a flow rate of 0.4 mL/min. For chromatographic separation a gradient starting from 98% to 85% solvent A within 20 min, to 20% within 19 min, to 0% within 4 min, and isocratic at 0% for 7 min was used. An electrospray ion source with the voltage of 3.5 kV, gas temperature of 200°C, a sheath gas temperature of 350°C and flow of 12 L/min was used. The full scan mass spectra ( $m/z$  75–3200) and spectra at collision energies (CE) 20 eV and 40 eV were measured in positive and negative ionisation mode. Putative identification (level 3) was performed by matching high resolution mass spectra with the Mass Hunter Metlin AM PCDL database (version 8.0, 79 609 compounds) and in-house amino acid metabolism database (250 compounds).

The raw data were converted using Mass Profiler Professional (MPP; version 12.1, Agilent Technologies, Agilent) and analysed by molecular feature extraction (Mass Hunter B.06.00, Agilent) as previously described (Errard et al., 2015).

Additionally, statistical software Prism 5 for Windows (Version 5.03; GraphPad Software, Inc.) was used (mean, standard deviation, Tukey's multiple comparisons test,  $p \leq 0.05$ ,  $n = 3$ ) to compare the relative changes in peaks areas of selected compounds (Figure 5).

## 3 | RESULTS

### 3.1 | Microscopic determination of MNP particles in pak choi

The aim of our study was to select a suitable method to detect the MNPs in plants. In our method, we used fluorescent particles of defined sizes (Supporting Information S1: Table S1) to track the particles in plant tissues using fluorescence microscopy. Tissues from plants grown under the same conditions, but without the administration of particles, were used as control samples to adjust the detector gain of the microscope. To be sure that the fluorescent

particles were detectable and stable over a period of 4 weeks, we compared freshly diluted 2  $\mu\text{m}$  PMMA particles with those stored for 4 weeks in  $\frac{1}{2}$  MS solution (Figure 1a,i-iv) and found no difference in the detectability including no change in shape, size and fluorescence. Considerably more interesting we were able to detect 2  $\mu\text{m}$  PMMA particles in the brightfield channel and were able to unambiguously assign the fluorescent dye in the fluorescence channel to the particle without any false positives or negatives in both control samples (particles on filter paper) and plant tissues (Figure 1b,c). This facilitates the interpretation of the results and provides a reproducible and reliable assessment of particles. However, for smaller particles (<200 nm), single particle detection was not possible due to the limitations of CLSM microscopy, but it is

possible to detect particle agglomerates (Supporting Information Material S1: Figure S3).

Using fluorescence and bright-field microscopy, we confirmed the assignment of the dye to MNPs and showed that our CLSM method is highly suitable for the detection of single particles  $\leq 2 \mu\text{m}$  in plant tissues.

### 3.2 | Uptake of NP from culture medium, solution, soil and after foliar application into pak choi

To determine if the uptake of NP depends on the way they are introduced into the environment, 401–450 nm fluorescent particles

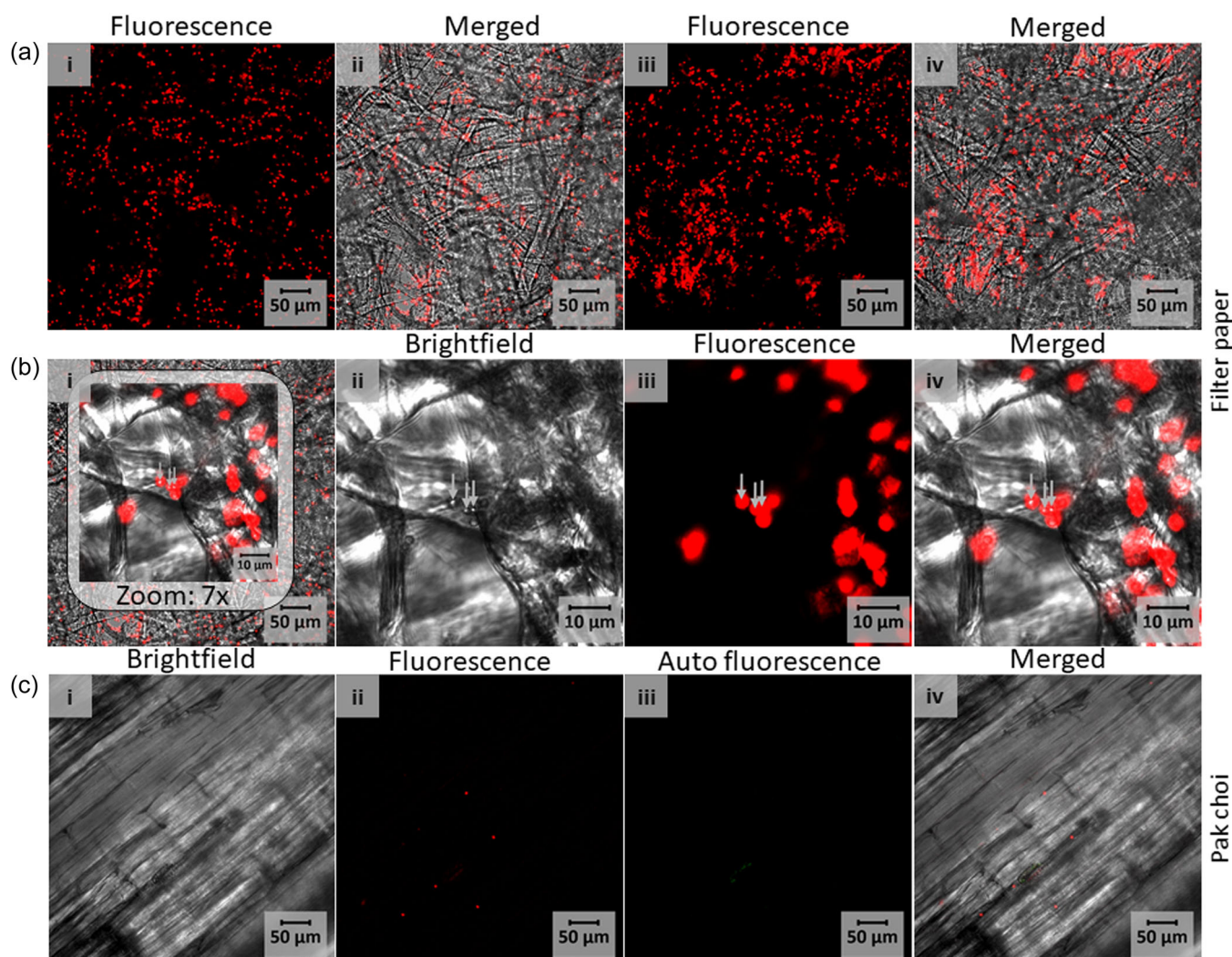


**FIGURE 1** Microscopic images of fluorescent 2  $\mu\text{m}$  PMMA MP COOH surface modified particles (red) on; (a) filter paper with freshly prepared particle solution diluted 1:8 with  $\frac{1}{2}$  Murashige-Skoog (MS,  $c_{\text{particles}} = 0.625 \text{ mg/mL}$ ) solution (i–ii) and the same solution on filter paper after 4 weeks (iii, iv). (b) different channels used for detection of the particles on paper are shown in i; merged picture zoom in (x7), ii; brightfield, iii; red fluorescence channel, iv; merged picture. (c) different channels used for detection of the particles in pak choi stem, grown in  $\frac{1}{2}$  MS medium with agar and with added particle solution ( $c_{\text{particles}} = 0.625 \text{ mg/mL}$ ) are shown in i; brightfield, ii; red fluorescence channel, iii; auto fluorescence channel, iv; merged picture. The particle fluorescence is shown in red ( $\lambda = 505\text{--}530 \text{ nm}$ ), auto fluorescence in green ( $\lambda \geq 505 \text{ nm}$ ), the grey arrows show particles. COOH, carboxylated; MP, microplastic particles; PMMA, poly(methyl methacrylate).

have been applied in different ways ( $\frac{1}{2}$  MS medium,  $\frac{1}{2}$  MS solution, soil and foliar uptake, Supporting Information S1: Figure S1).  $\frac{1}{2}$  MS medium was used to ensure optimal plant growth and to improve the comparability of results. The particles were taken up by the vegetables *via* the roots and translocated to the stem (in particular the xylem) and the leaves. Also, the fluorescence signals from the particles were detected in the intercellular space and in the vasculature system of stem and leaves mid rib (Figure 2, Supporting Information Material S1: Figure S4), whereas no signal has been detected in leaves. The presence of particles in treated pak choi roots grown in  $\frac{1}{2}$  MS solution and soil, has been observed on the root surface in maturation and in lateral root primordium (Figure 3a,b and Supporting Information Material S1: Figure S4). NP particles were observed in the stem of plants after uptake *via* the roots from  $\frac{1}{2}$  MS solution and soil (Figure 3a,b); however, no particles were found in the leaves under our experimental conditions. After the application of 401–450 nm particles to the leaf surface, they could be detected in the cuticle of the upper epidermis of the leaves (adaxial) even after careful washing before microscopic observation. The penetration of particles into the leaf was confirmed by the fluorescence signals in the midrib following a transect cut. The particles have been distributed mainly in the intercellular space and the plant's vasculature system (Figure 3c). It has to be mentioned that there was no auto fluorescence in the control samples (sprayed with  $\frac{1}{2}$  MS solution); therefore, we had no effect on the fluorescence signals of the particles in leaf samples exposed with 401–450 nm particles.

In conclusion, the uptake of NP into pak choi and their translocation in the plant can occur *via* the root and *via* the leaves and has been demonstrated by the utilisation of different model systems ( $\frac{1}{2}$  MS medium,  $\frac{1}{2}$  MS solution, soil and foliar application). None of the examined plants displayed any visible alterations.

### 3.3 | Influence of particle size and surface modification on the uptake in pak choi

To assess whether NP with different size and surface modification can be taken up differently by the plants, PS-COOH, PS-NH<sub>2</sub> or PS-plain fluorescence labelled particles with two different sizes (100 and 500 nm) were added to the  $\frac{1}{2}$  MS medium. As shown in Supporting Information S1: Figure S4A–F, PS particles regardless of their size and surface modification have entered and translocated in pak choi plants grown in  $\frac{1}{2}$  MS medium. However, there were increased fluorescent signals observed in 100 nm size PS particles compared to the 500 nm. PS particles (all surface modifications and sizes) entered mostly *via* the lateral root primordia to the root stele and have been observed in the stem and leaves vascular system. A few signals have been obtained in the root tip for PS-plain and PS-NH<sub>2</sub> surface modification, but there were no signals for PS-COOH particles. Furthermore, in stem the PS particles despite their size and surface modification accumulated in intercellular spaces. No fluorescence signals have been detected in the control samples (Supporting Information Material S1: Figure S4).

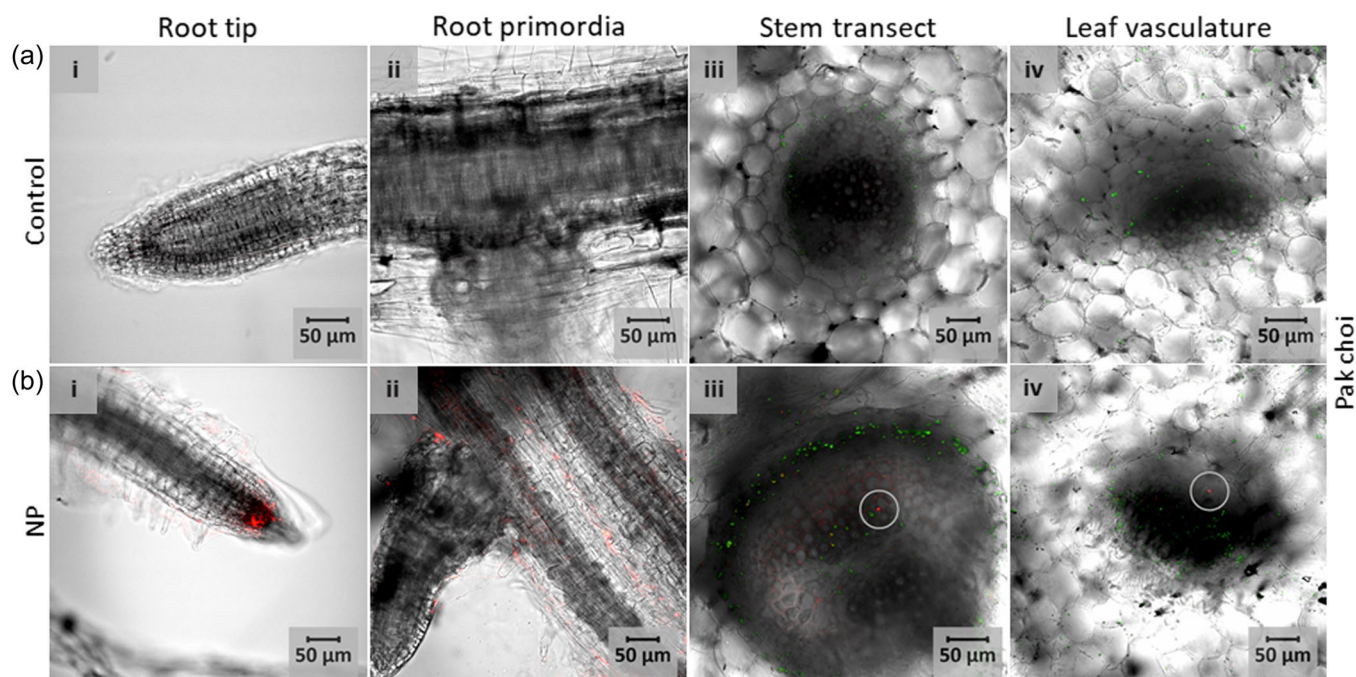


**FIGURE 2** Translocation of 401–450 nm PMMA NP COOH (carboxylated) in pak choi in  $\frac{1}{2}$  Murashige-Skoog medium with agar; (a, b) (i) lateral root tip, (ii) root primordia, (iii) stem transect, (a) shows the control samples and (b) shows the samples exposed to PMMA NP. The particle fluorescence is shown in red ( $\lambda = 505\text{--}530$  nm), auto fluorescence in green ( $\lambda \geq 505$  nm), grey circles indicate particles. COOH, carboxylated; NP, nanoplastic particles; PMMA, poly(methyl methacrylate). [Color figure can be viewed at [wileyonlinelibrary.com](https://onlinelibrary.wiley.com/doi/10.1111/pce.15115)]

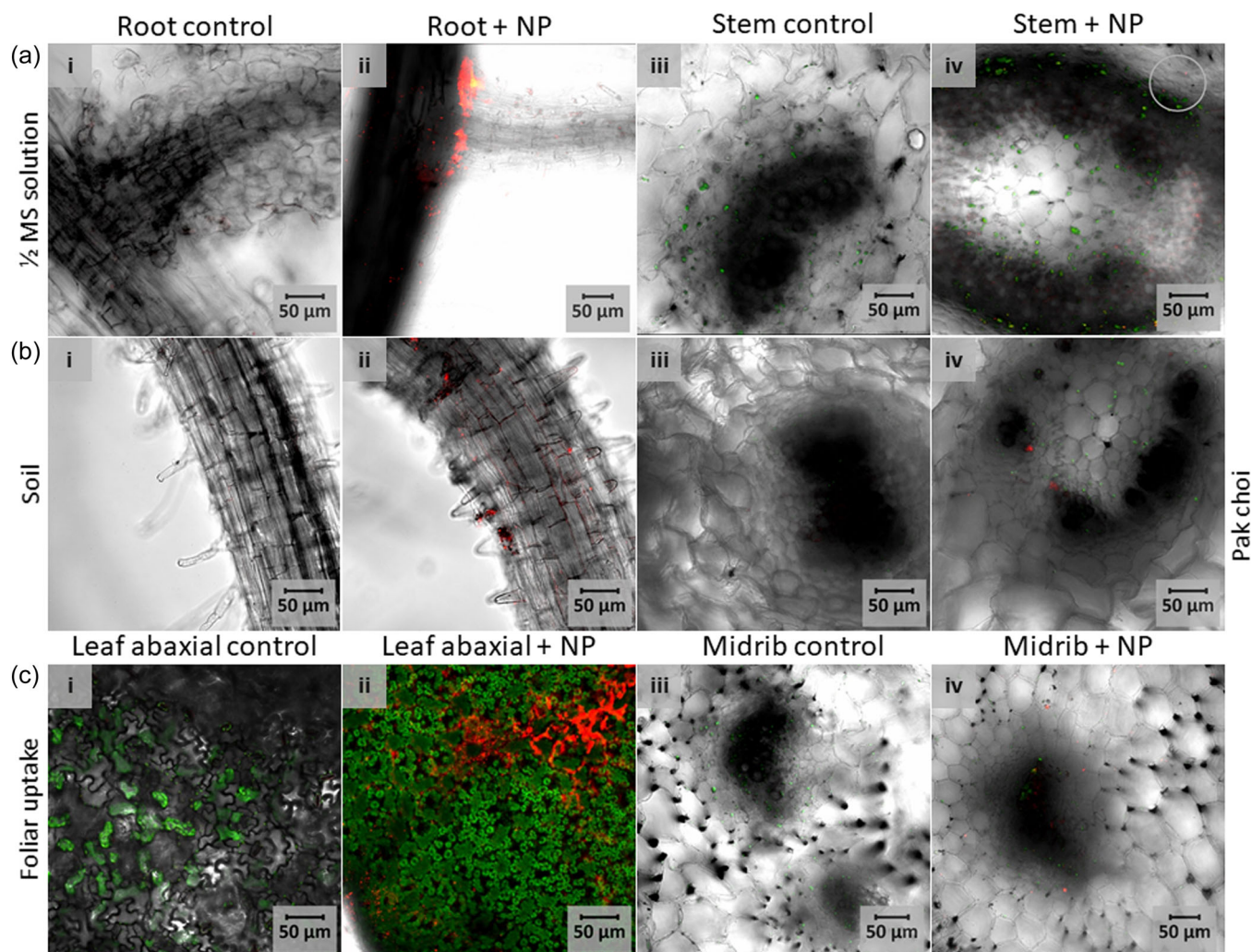


**FIGURE 3** Microscopic pictures of pak choi plants treated with 401–450 nm PMMA NP COOH (carboxylated),  $\frac{1}{2}$  MS simulating different ways of uptake, (a)  $\frac{1}{2}$  Murashige-Skoog (MS) solution: i, ii, particles concentrated to lateral root primordia surface and iii, iv, particles in stem. (b) soil: i, ii, particles sticking on root surface and entry via small injuries and iii, iv, particles in stem. (c) foliar application: i, adaxial application of 4  $\mu$ L of  $\frac{1}{2}$  MS solution to leaf as control; ii, adaxial application of 4  $\mu$ L of freshly prepared particle solution diluted 1:4 with  $\frac{1}{2}$  MS solution ( $c_{\text{particles}} = 1.25$  mg/mL) to leaf; iii, midrib control; iv, adaxial entry of particle into leaf midrib. The particle fluorescence is shown in red ( $\lambda = 505\text{--}530$  nm), auto fluorescence in green ( $\lambda \geq 505$  nm), the grey circles indicate particles. COOH, carboxylated; NP, nanoplastic particles; PMMA, poly (methyl methacrylate). [Color figure can be viewed at [wileyonlinelibrary.com](https://onlinelibrary.wiley.com/doi/10.1111/pcel.13653)]

### 3.4 | NP in different edible parts of vegetables

To determine whether NP can be taken up by edible parts of vegetables; asparagus, radish, pak choi plants have been exposed to 401–450 nm PMMA particles and tomato plants subjected to 500 nm PS-COOH modified surface in  $\frac{1}{2}$  MS medium. No fluorescence signal was observed in root, stem and leaf specimens of control samples from all targeted vegetables (Figures 2 and 4). Red fluorescent signals of PMMA particles have been detected mainly on the root surface, in endodermis and xylem of asparagus plants. Once 401–450 nm PMMA particles entered the vasculature, they translocated from the roots to the vascular bundle in stem also to ground tissue and chlorenchyma from intercellular spaces (Figure 4b,i–iv). CLSM observations have confirmed the entry of 401–450 nm PMMA particles into internal root structure especially in maturation region of

radish plants. It has to be mentioned, despite washing the roots before the specimen preparation, particles aggregations on root surface have been observed. Though, the particles have been detected mostly attached to the surface, their accumulation seems to be higher in root maturation region than the root tip (Figure 4b,i,ii,d,i,ii). Similar to the observation for the stem in asparagus, the 401–450 nm PMMA particles accumulated in stem collenchyma and vascular bundle of treated radish plants (Figure 4d,iii). In addition, particles further translocated to the leaf vascular bundle and intercellular spaces (Figure 4d,iv). The same entry and translocation patterns have been seen in pak choi plants treated with 401–450 nm PMMA particles (Figure 2b,i–iv). In a follow up experiment with tomato plants grown in soil we have applied the 500 nm PS-COOH particles and interestingly, the particles (purple fluorescence) accumulated in the fruit's mesocarp and placenta (Figure 4e).

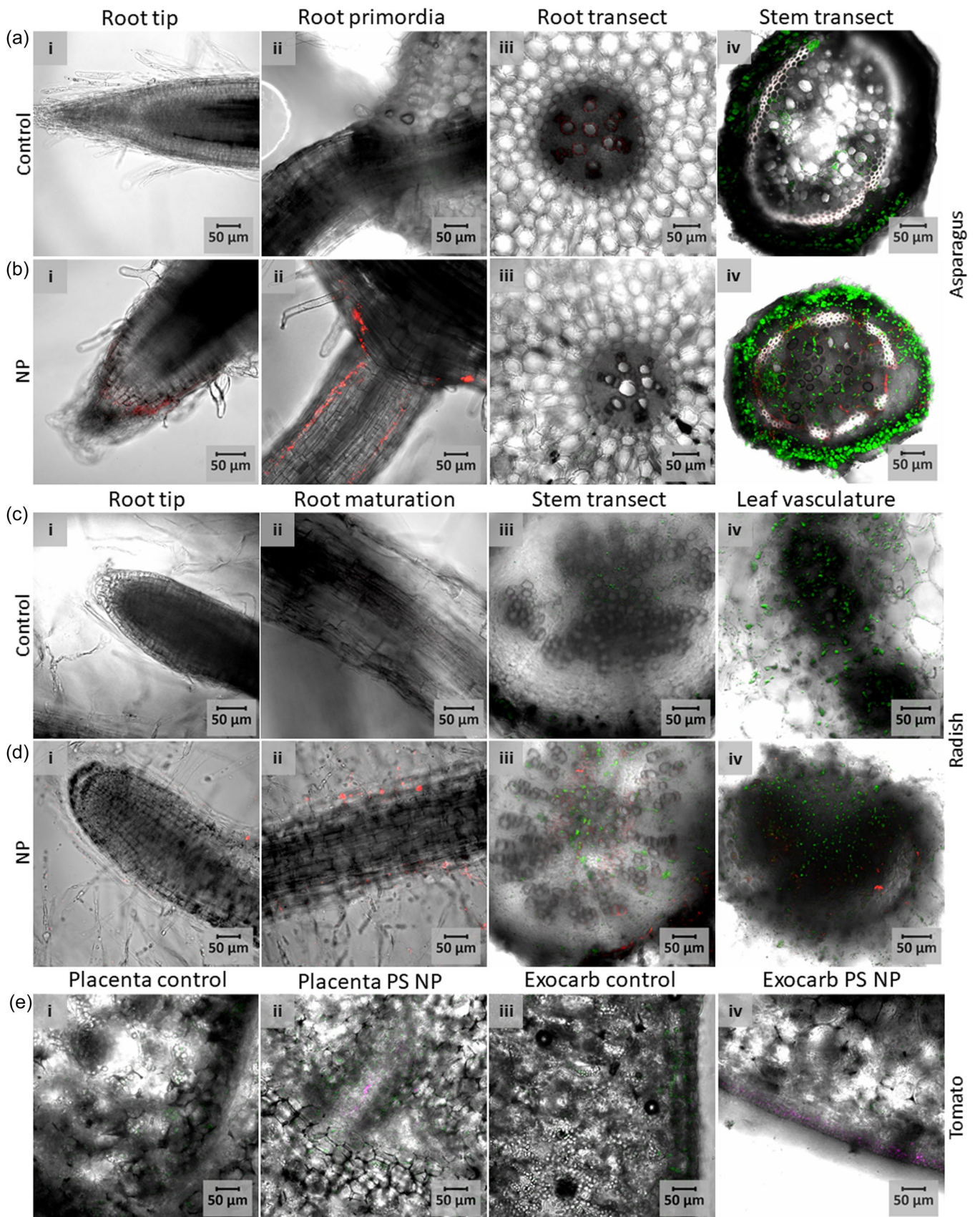


FIGURE 4 (See caption on next page).

### 3.5 | Effect of NP on pak choi plant's metabolome

UHPLC-Q-TOF-MS was used to evaluate the effect of 401–450 nm PMMA-COOH surface modified particles on metabolic induce changes in pak choi plants, thereafter; the results processed by multivariate data analysis and visualised using principal component analysis (Figure 5a,b). There was a clear discrimination between plants treated with PMMA particles of 401–450 nm and the control group (Figure 5a,b). The metabolic profiling indicated 401–450 nm PMMA particles application caused significant changes mainly in phenolic compounds, phospholipids and phytohormone derivatives between the control and the treated samples (Figure 5c). Among the phenolic compounds there were some increased in response to PMMA treatment, for instance, three hydroxycinnamic acid compounds abundance (1-O-p-coumaroyl-( $\beta$ -D-glucose 6-O-sulfate), trans-o-coumaric acid 2-glucoside, okanin 4-methyl ether 4'-O-(2"-O-caffeoyl-6"-O-acetylglucoside) also isorhamnetin 3-glucuronide-7-sulfate, quercetin 3-(2"-feruloylsophoroside) and a kaempferol based compound (kaempferol 7,4'-dimethyl ether 3-O-sulfate) induced in both root and stem in treated samples. The same trend has been observed in some phytohormone derivative levels (Figure 5c). Interestingly, PMMA remarkably decreased some phenolic compounds level such as; dihydrocaffeic acid 3-O-glucuronide, and kaempferol 7-methyl ether 3-(6-(E)-3,5-dimethoxy-4-hydroxycinnamoylglucosyl)-(1-2)-[rhamnosyl-(1-6)-glucoside] in the roots of treated samples. (Figure 5). Having a closer look showed that most of the anionic phospholipids with bilayer structure (phosphatidic acid, phosphatidylinositol and phosphatidylglycerol) have been detected in lower concentrations in roots treated with 401–450 nm PMMA but there were no significant changes observed in stems expected of an increase in phosphatidic acid concentrations in treated stems. A significant increase was shown in non-bilayer phospholipids in the treated roots (Figure 5). A comparison of the fresh weight of the roots and shoots of the treated and control plants revealed no significant differences (Supporting Information Material S1: Figure S5).

## 4 | DISCUSSION

### 4.1 | Using fluorescent MNPs for translocation studies in plants

Previous microscopic studies on MNPs entry to plants shows limitations of instrumental methodology for detection of MNPs specifically in photosynthetic organisms, therefore some parameters as a

whole for visual slide evaluation needs to be optimised (Larue et al., 2021). Image resolution, auto fluorescence noise in background of images and more precise localisation of MNPs in different plant tissues are such parameters (Mariano et al., 2021). The application of SEM or scanning transmission electron microscopy (STEM) as a supplementary method for the localisation of MNPs in the plant can be employed when the MNPs are doped with metal ions such as Pd or Eu (Luo et al., 2022; Sun et al., 2020). In the absence of such doping, however, the particles are indistinguishable from natural, round-shaped molecules, such as polysaccharide granules or spores, due to the high carbon content of the polymers and the plant material. This is because SEM and STEM only provide information about the elemental composition and the morphology (Schwaferts et al., 2019). For the identification of MNPs,  $\mu$ -FTIR could be an option, but was not deemed suitable for our study due to its inability to detect particles below 20  $\mu$ m (Ivleva et al., 2017). Our microscopic method using fluorescent MNPs with defined size confirmed stability and reliability of our detection method. The fluorescence signal after 4 weeks provided sufficient signal for detection. Our microscopic images show the strength of detection of MNPs *in planta*. The observed uptake and distribution of NP in pak choi plants is mostly similar to the published results on wheat and lettuce plants (Li, Luo, Peijnenburg, et al., 2020; Li et al., 2020). Nonetheless, our technique eliminates the need for differential staining of particles with fluorescent dyes, because at particle sizes > 2  $\mu$ m the particles can be detected in brightfield. Distribution effects result in the dilution of MNPs load in the upper parts of the plants. Therefore, it is essential to detect and locate individual particles, which was shown in this study. The method described cannot avoid the shielding effects caused by the strong auto fluorescence in the leaves (Azeem et al., 2021). However, the detection of particles in the leaf midrib suggests that they are transported further into the leaves and accumulate there. Several experimental repetitions were conducted to distinguish particle fluorescence from auto fluorescence in the experiments. For more precise localisation in plant tissues, advanced microscopic techniques including supportive software tools should be used in future studies.

### 4.2 | Pak choi plants uptake MNPs from different ways of administration

We have applied 401–450 nm PMMA particles in different ways to see if the penetration of particles depends on the way plants are

**FIGURE 4** Translocation of 401–450 nm PMMA NP COOH (carboxylated) in edible part of; (a, b) asparagus (i) lateral root primordia (ii) transverse section of root (iii) transverse section of shoot, (a) shows the control samples and (b) shows the samples exposed to PMMA NP; (c, d) radish (i) root tip, (ii) root maturation region (iii) transverse section of stem, (iv) transverse cut of midrib. (c) shows the control samples and (d) shows the samples exposed to PMMA NP. The PMMA NP fluorescence is shown in red ( $\lambda = 505\text{--}530$  nm), auto fluorescence in green ( $\lambda \geq 505$  nm). Translocation of 500 nm PS NP COOH (carboxylated) in edible part of; (e) tomato (i) mesocarp control, (ii) mesocarp PS NP, (iii) placenta control, (iv) placenta PS NP. The PS NP fluorescence is shown in purple ( $\lambda = 505\text{--}530$  nm), auto fluorescence in green ( $\lambda \geq 505$  nm). COOH, carboxylated; NP, nanoplastic particles; PMMA, poly (methyl methacrylate). [Color figure can be viewed at [wileyonlinelibrary.com](https://onlinelibrary.wiley.com)]

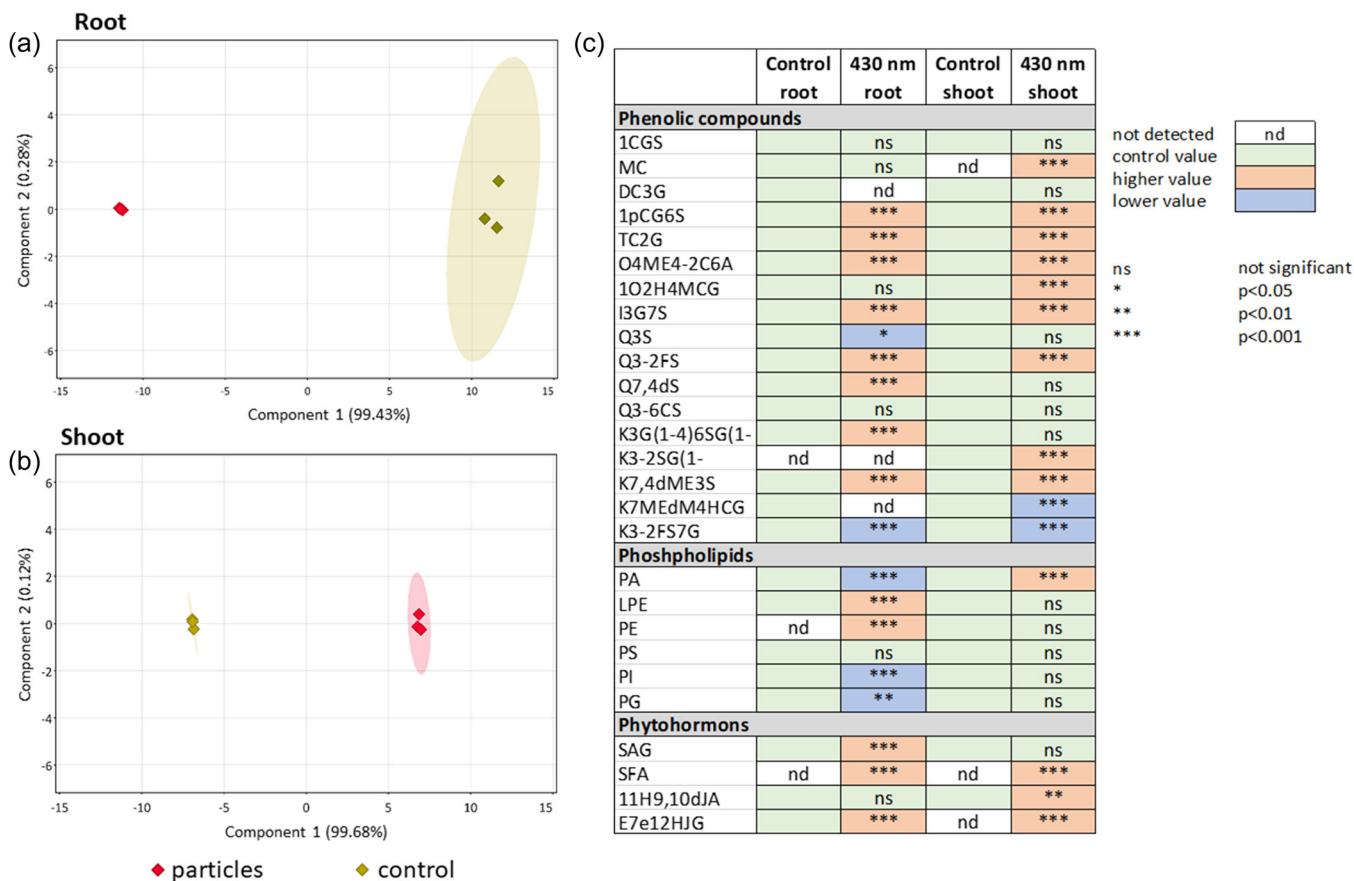


**FIGURE 5** Metabolomic changes due to PMMA NP treatment in pak choi. (a) Principal component analysis (PCA) of PMMA NP treated (red) versus control plants (ochre) in pak choi roots, (b) PCA of PMMA NP treated (red) versus control plants (ochre) in pak choi shoots, (c) Up- and downregulation of tentatively identified compounds in roots and shoots of PMMA NP treated versus control plants in pak choi (1CGS, 1-O-caffeoyl-(β-D-glucose 6-O-sulfate); MC, methyl caffeate; DC3G, dihydrocaffeic acid 3-O-glucuronide; 1pCG6S, 1-O-p-coumaroyl-(β-D-glucose 6-O-sulfate); TC2G, trans-o-coumaric acid 2-glucoside, O4ME4-2C6A, okanin 4-methyl ether 4'-O-(2"-O-caffeoyl-6"-O-acetylglucoside); 1O2H4MCG, 1-O-2'-hydroxy-4'-methoxycinnamoyl-β-D-glucose; I3G7S, isorhamnetin 3-glucuronide-7-sulfate; Q3S, quercetin 3-sophorotrioside; Q3-2FS, quercetin 3-(2"-feruloylsphoroside); Q7,4dS, quercetin 7,4'-disulfate; Q3-6CS, quercetin 3-(6"-caffeoylsphoroside); K3G(1-4)6SG(1-2)G, kaempferol 3-glucosyl-(1-4)(6"-sinapylglucosyl)(1-2)-galactoside; K3-2SG(1-4)6SG(1-2)G, kaempferol 3-(2"-sinapylglucosyl)(1-4)(6"-sinapylglucosyl)(1-2)-galactoside; K7,4dME3S, kaempferol 7,4'-dimethyl ether 3-O-sulfate; K7MEdM4HCG, kaempferol 7-methyl ether 3-(6-(E)-3,5-dimethoxy-4-hydroxycinnamoylglucosyl)-(1-2)-[rhamnonyl-(1-6)-glucoside]; K3-2FS7G, kaempferol 3-[2"--(E)-feruloylsphoroside]-7-glucoside; LPE, lysophosphatidylethanolamine; PA, phosphatidic acid; PE, phosphatidylethanolamine; PG, phosphatidylglycerol; PI, phosphatidylinositol; PS, phosphatidylserine; SAG, salicylic acid β-D-glucoside; SFA, salicyfolioside A; 11H9,10dJA, (-)-11-hydroxy-9,10-dihydrojasmonic; E7e12HJG, ethyl 7-epi-12-hydroxyjasmonate glucoside). [Color figure can be viewed at [wileyonlinelibrary.com](http://wileyonlinelibrary.com)]

exposed to MNPs' pollution. Pak choi plants could uptake PMMA NP from ½ MS medium, solution and soil mainly by the lateral roots in maturation region. The root exudate and mucilage from the border cells of root tip can act as a barrier to prevent plants root to uptake MNPs (Wu et al., 2021). Our results provided clear evidence of lateral root primordia as a potential MNPs entry site. Particles enter the plants root via cracks formed by protrusion of lateral roots when primordia grow out from the root cortex (Li, Luo, Peijnenburg, et al., 2020). These cracks can be formed due to mechanical pressure from surrounding tissues (Banda et al., 2019). This mechanism is similar to the bacterial entry to the plants root described in previous studies (Goormachtig et al., 2004; Kong et al., 2020). Subsequently, PMMA nanoplastics moved from the root xylem to the stem

vasculature of treated pak choi plants through intercellular space via the apoplastic pathway, which is in agreement with the results from recent studies (Li, Luo, Peijnenburg, et al., 2020; Liu et al., 2022; Sun et al., 2020). Symplastic pathway also mediates transportation from NP for their cell-to-cell movement of particles via plasmodesmata or endocytosis (Etxeberria et al., 2006; Rong et al., 2024). MNPs can move into endodermis region from the intercellular space by liquid phase endocytosis (Liu et al., 2022; Maity et al., 2022). Our observations of the PMMA NP translocation into leaf vasculature of plants grown in ½ MS medium could be because of better root development due to the less external stimuli in solid MS medium (Sun et al., 2020). Our CLSM observations showed accumulation of particles in intercellular space of pak choi stem where then they can be pulled to the

leaf vascular bundle *via* transpiration stream as a major force for their migration (Li, Luo, Peijnenburg, et al., 2020; Liu et al., 2022).

Foliar application of PMMA particles on leaves were trapped by the cuticle and absorb mainly *via* stomatal opening. Consequently, the particles translocated into vascular system, which is in accordance to literature (Larue et al., 2014; Li, Gao, et al., 2021; Li, Li, et al., 2021; Sun et al., 2022; Xiong et al., 2017). The presence of particles in leaf vascular system and intercellular spaces in our experiment is in good accordance with the literature, where they also confirmed the entry and translocation of PS nanoplastics regardless of their surface charge/modification (Li, Gao, et al., 2021). Despite washing the leaves before specimen preparation, there was an aggregation of PMMA NPs on the adaxial surface of the leaf which was microscopically indistinguishable from the unwashed samples. This demonstrates that washing does only minimally reduce or not reduce the PMMA content on the leaf surface, which has been previously observed for Ag NPs (approximately 40 nm) on lettuce plants (Larue et al., 2014).

In summary, this study shows that NP can enter and distribute within plants.

#### 4.3 | Pak choi plants uptake PS NP regardless of their size and surface modification

In this study, pak choi plants were exposed to 100 and 500 nm PS particles with amino groups (-NH<sub>2</sub>), carboxy groups (-COOH), and neutral surfaces. The plants were able to take up particles regardless of their size or surface modification. In contrast to our findings, the entry and translocation of PS particles with different size and surface charge/modification was reported to be different. For instance, PS-COOH particles in both sizes did not adhere to the root tip which is likely due to electrostatic repulsion between negatively coated PS particles and negatively charged root cell wall, conversely, aggregation of positively charged 500 nm PS-NH<sub>2</sub> NP in ½ MS medium could be to electrostatic attraction (Sun, Lei et al., 2021; Sun, Wang et al., 2021). Furthermore, positively charged NP stimulates root exudation which in return, enhances the aggregation of particles on the root surface (Sun et al., 2020). Regarding the active cell division in root cap cells, the particles diffused through the apical meristem tissue through the epidermal layers where Casparian strip is not fully developed (Li, Luo, Peijnenburg, et al., 2020; Roy et al., 2023). PS-COOH particles could thus have been penetrated the root surface and enter to the root stele by likely polyvalent cation bridges formation. From where they later have move to the plant's aerial parts by the apoplastic pathway through the transpiration flow (Dong et al., 2021; Liu et al., 2022; Sun, Lei et al., 2021). The accumulation of PS NP in the intercellular spaces can be attributed to hydrophobic interactions between the conjugated C = C side chains of lignin in the cell walls and the phenolic groups of the PS NP (Sun, Wang et al., 2021). Given that the particles in our experiments were discovered in the vascular system and intercellular spaces of various plant parts (roots, stems, and leaf midribs) regardless of surface

modifications, it can be inferred that the aforementioned effects have minimal impact on particle uptake and translocation. Further research is needed to investigate the varying intensity of electrostatic effects of particles on uptake and distribution processes, which is influenced by the charge to surface ratio as well as surface depositions in natural environments (Shi et al., 2024).

#### 4.4 | NP accumulate in edible part of vegetables, a risk assessment for food safety

Our study clearly provides evidence of accumulation of NP in the edible parts of the targeted vegetables (asparagus, radish, pak choi and tomato) which indicates the entry of NP to food chain and in consequence its potential effect on human health (Rose et al., 2023). Accumulated particles in intercellular spaces moved through the xylem *via* apoplastic pathway and were further transported through transpiration, as already described above. Another explanation of the NP entry to the cell could be the lower mechanical strength (Young's modulus) of PS (2.1 GPa) and PMMA (2.9 GPa) compared to the cell wall (130 GPa roughly), which caused deformation of the particles while entering the cell and facilitated the migration of PS and PMMA particles in our study to edible tissues (Dong et al., 2021; Gibson, 2012). Recent studies reported the entry and accumulation of MNPs in different leafy vegetables (garden cress and lettuce) which are in good agreement with our findings with pak choi plants (Bosker et al., 2019; Lian et al., 2021). White asparagus is grown naturally under soil covered by plastic mulch films to prevent photosynthesis and produce milky white spears. Regarding the fact that plastic mulching is a major source to produce MNPs in agricultural soils, asparagus plants are exposed to high risk of MNPs entry coming both from soil or plastic films degradation (Pérez-Reverón et al., 2022). Radish roots with storage function are in direct contact with MNPs and therefore can be a risk to humans, too. Our finding of the accumulation of NP in radish roots is in consistence with the literature (Tympa et al., 2021). For the first time, we reported the accumulation of NP in tomato fruits which indicates effective absorption of PS particles by roots and consequently their high upward (root to shoot) transportation within the vascular system.

#### 4.5 | NP change metabolite composition in pak choi plants treated with PMMA particles

Our metabolomics study showed treating pak choi plants with PMMA 401–430 nm stimulated the roots to produce high levels of phenolic compounds, which can be a response of treated plants to adapt to the stressful environment (Dong et al., 2021). Metabolic profile alterations and increased phenolic compounds levels in rice plants exposed to PS NP have been previously reported, which is in line with our findings (Wu et al., 2021). However, some phenolic compounds have been decreased significantly in treated plants, which could be because of stimulation of

the root exudates by particle's entry which modulates the secondary metabolite's profiles in response to NP uptake (Neugart et al., 2018). Interestingly, we found that the level of bilayer phospholipids such as phosphatidic acid in both shoot and root, and phosphatidylglycerol and phosphatidylinositol in roots, were reduced in response to PMMA uptake by pak choi. Nonbilayer phospholipids (lysophosphatidylethanolamine [LPE] and phosphatidylethanolamine [PE]), by contrast, have been increased in pak choi roots treated with PMMA. Alterations in the relative amounts of non-bilayer lipids have been observed in plants in response to different environmental stresses such as salt, drought and high light (Darwish et al., 2009; Harwood, 1998). Lysophospholipids are present in trace amounts in biological membranes and their levels dramatically changes upon exposure of plants to biotic and abiotic stimuli (Cowan, 2009). Induced signalling and biosynthesis gene expression of the defensive hormone salicylic acid (SA) in *Arabidopsis* plants treated with LPE has been reported (Völz et al., 2021). They indicated that LPE acts as an immunity-promoting agent which activates a wide range of defence-related-traits associated with SA metabolism and H<sub>2</sub>O<sub>2</sub> turnover. The increase in LPE levels in the roots of pak choi plants treated with PMMA may indicate that PMMA causes stress in plants upon entry to the roots. As a result, the plant induces LPE levels, which are associated with inducing SA metabolism. Disturbance of root metabolic activities and physiological function in pumpkin plants treated by iron oxide nano- and microparticles and local instability of the cell membrane lipid bilayer has been previously reported (Wang et al., 2011). We propose that the non-bilayer phospholipids has lower surface tension than bilayer phospholipids with a rather tightly closed surface, which allows the penetration of the NP into the cell membrane, which could be one of the mechanisms plants use to adapt to the stressful environment and a reason how NP in our experiment could move upward through the plant (Garab et al., 2016). PMMA remarkably increased the content of SA beta-D-glucoside (SAG); a storage form of a defence signal against biotic and abiotic stresses in plants and ethyl 7-epi-12-hydroxyjasmonate glucoside (E7e12HJG); a jasmonic acid derivative (Kawano et al., 2004). It has been reported that SA and jasmonic acid act as signalling molecules in response to different biotic and abiotic plant stresses (Janda et al., 2020; Ruan et al., 2019). Alterations in signalling phytohormones level in response to NP entry could be an indication that NP act as abiotic stress and increases JA and SA concentrations in pak choi plants as previously described in rice plants treated with PS NP (Wu et al., 2021). Moreover, JA activates phenolic biosynthetic pathway via stimulating the activity of the phenylalanine ammonia lyase. The same relationship have been defined between SA and flavonoid accumulation after changing the nutrient supply (Neugart et al., 2018; Parween & Jan, 2020). The impaired uptake of nutrients by roots blocked with MNPs can also result in a change in the metabolome (Jiang et al., 2019). The growth of root and shoot was due to the short treatment time of 4 days not significantly affected (Supporting Information Material S1: Figure S5), which is in accordance to a study with garden cress (Bosker et al., 2019). In fact, our metabolomic result suggests that NP can alter the plant metabolome by modulating different pathways in treated plants, although further studies are needed for a more detailed conclusion.

## 5 | CONCLUSION

Our findings of NP entry to edible parts of vegetables (asparagus: root, pak choi: leafy vegetable and tomato: fruit) highlight the risk of human exposure to NP through the consumption of contaminated vegetables and emphasise the need for more investigations on the impact of NP on food safety and quality as well as potentially for human health. Further analytical methods need to be developed and established to provide quantitative information on the distribution and transport of NP in plants. It is necessary to assess the risk of NP entering the food chain through crops and to establish new management strategies to control the release of plastic waste particles into the terrestrial environment.

## ACKNOWLEDGEMENTS

The authors would like to thank the technical assistance at IGZ for the help and technical support. This project was funded by the by EFRE funds (funding number: 85037644) from the Investitionsbank des Landes Brandenburg (ILB).

## CONFLICT OF INTEREST STATEMENT

The authors declare no conflict of interest.

## DATA AVAILABILITY STATEMENT

The data that support the findings of this study are available from the corresponding author upon reasonable request.

## ORCID

Eric Zytowski  <http://orcid.org/0009-0002-2164-6858>

Susanne Baldermann  <https://orcid.org/0000-0002-1501-4320>

## REFERENCES

- Andrady, A.L. & Neal, M.A. (2009) Applications and societal benefits of plastics. *Philosophical Transactions of the Royal Society, B: Biological Sciences*, 364, 1977–1984. <https://doi.org/10.1098/rstb.2008.0304>
- Azeem, I., Adeel, M., Ahmad, M.A., Shakoor, N., Jiangcuo, G.D., Azeem, K. et al. (2021) Uptake and accumulation of nano/microplastics in plants: a critical review. *Nanomaterials*, 11, 2935. <https://doi.org/10.3390/nano11112935>
- Banda, J., Bellande, K., von Wangenheim, D., Goh, T., Guyomarç'h, S., Laplaze, L. et al. (2019) Lateral root formation in *Arabidopsis*: a well-ordered L-Rexit. *Trends in Plant Science*, 24, 826–839. <https://doi.org/10.1016/j.tplants.2019.06.015>
- Bosker, T., Bouwman, L.J., Brun, N.R., Behrens, P. & Vijver, M.G. (2019) Microplastics accumulate on pores in seed capsule and delay germination and root growth of the terrestrial vascular plant *Lepidium sativum*. *Chemosphere*, 226, 774–781. <https://doi.org/10.1016/j.chemosphere.2019.03.163>
- Braun, U., Eisentraut, P., Altmann, K., Kittner, M., Dümichen, E., Thaxton, K. et al. (2020) Accelerated determination of microplastics in environmental samples using Thermal Extraction Desorption-Gas Chromatography/Mass Spectrometry (TED-GC/MS) [WWW Document], Agilent Technologies Application Note Environmental. <https://www.agilent.com/cs/library/applications/application-microplastics-determination-by-ted-gc-msd-5994-2551en-agilent.pdf>
- Cowan, A.K. (2009) Plant growth promotion by 18:0-lyso-phosphatidylethanolamine involves senescence delay. *Plant Signaling & Behavior*, 4, 324–327. <https://doi.org/10.4161/psb.4.4.8188>

- Darwish, E., Testerink, C., Khalil, M., El-Shihy, O. & Munnik, T. (2009) Phospholipid signaling responses in salt-stressed rice leaves. *Plant and Cell Physiology*, 50, 986–997. <https://doi.org/10.1093/pcp/pcp051>
- Dong, Y., Gao, M., Qiu, W. & Song, Z. (2021) Uptake of microplastics by carrots in presence of as (III): combined toxic effects. *Journal of Hazardous Materials*, 411, 125055. <https://doi.org/10.1016/j.jhazmat.2021.125055>
- Duemichen, E., Eisentraut, P., Celina, M. & Braun, U. (2019) Automated thermal extraction-desorption gas chromatography mass spectrometry: a multifunctional tool for comprehensive characterization of polymers and their degradation products. *Journal of Chromatography A*, 1592, 133–142. <https://doi.org/10.1016/j.chroma.2019.01.033>
- Duis, K. & Coors, A. (2016) Microplastics in the aquatic and terrestrial environment: sources (with a specific focus on personal care products), fate and effects. *Environmental Sciences Europe*, 28, 2. <https://doi.org/10.1186/s12302-015-0069-y>
- Errard, A., Ulrichs, C., Kühne, S., Mewis, I., Drungowski, M., Schreiner, M. et al. (2015) Single- versus multiple-pest infestation affects differently the biochemistry of tomato (*Solanum lycopersicum* 'Ailsa Craig'). *Journal of Agricultural and Food Chemistry*, 63, 10103–10111. <https://doi.org/10.1021/acs.jafc.5b03884>
- Ettxeberria, E., Gonzalez, P., Baroja-Fernández, E. & Romero, J.P. (2006) Fluid phase endocytic uptake of artificial nano-spheres and fluorescent quantum dots by sycamore cultured cells: evidence for the distribution of solutes to different intracellular compartments. *Plant Signaling & Behavior*, 1, 196–200. <https://doi.org/10.4161/psb.1.4.3142>
- Garab, G., Ughy, B. & Goss, R. (2016) Role of MGDG and non-bilayer lipid phases in the structure and dynamics of chloroplast thylakoid membranes. In: Nakamura, Y. & Li-Beisson, Y., Eds *Subcellular Biochemistry*. Cham: Springer International Publishing. pp. 127–157. [https://doi.org/10.1007/978-3-319-25979-6\\_6](https://doi.org/10.1007/978-3-319-25979-6_6)
- Gaylarde, C.C., Baptista Neto, J.A. & da Fonseca, E.M. (2021) Nanoplastics in aquatic systems—Are they more hazardous than microplastics? *Environmental Pollution*, 272, 115950. <https://doi.org/10.1016/j.envpol.2020.115950>
- Gibson, L.J. (2012) The hierarchical structure and mechanics of plant materials. *Journal of the Royal Society Interface*, 9, 2749–2766. <https://doi.org/10.1098/rsif.2012.0341>
- Goormachtig, S., Capoen, W., James, E.K. & Holsters, M. (2004) Switch from intracellular to intercellular invasion during water stress-tolerant legume nodulation. *Proceedings of the National Academy of Sciences*, 101, 6303–6308. <https://doi.org/10.1073/pnas.0401540101>
- Hartmann, N.B., Hüffer, T., Thompson, R.C., Hassellöv, M., Verschoor, A., Daugaard, A.E. et al. (2019) Are we speaking the same language? recommendations for a definition and categorization framework for plastic debris. *Environmental Science & Technology*, 53, 1039–1047. <https://doi.org/10.1021/acs.est.8b05297>
- Harwood, J.L. (1998) Involvement of chloroplast lipids in the reaction of plants submitted to stress. In: Paul-André, S. & Norio, M., Eds *Lipids in Photosynthesis: Structure, Function and Genetics*. Springer Netherlands. Dordrecht. pp. 287–302. [https://doi.org/10.1007/0-306-48087-5\\_15](https://doi.org/10.1007/0-306-48087-5_15)
- Hua, Z., Ma, S., Ouyang, Z., Liu, P., Qiang, H. & Guo, X. (2023) The review of nanoplastics in plants: detection, analysis, uptake, migration and risk. *TrAC, Trends in Analytical Chemistry*, 158116889. <https://doi.org/10.1016/j.trac.2022.116889>
- Ivleva, N.P., Wiesheu, A.C. & Niessner, R. (2017) Microplastic in aquatic ecosystems. *Angewandte Chemie International Edition*, 56, 1720–1739. <https://doi.org/10.1002/anie.201606957>
- Janda, T., Szalai, G. & Pál, M. (2020) Salicylic acid signalling in plants. *International Journal of Molecular Sciences*, 21, 2655. <https://doi.org/10.3390/ijms21072655>
- Jiang, X., Chen, H., Liao, Y., Ye, Z., Li, M. & Klobučar, G. (2019) Ecotoxicity and genotoxicity of polystyrene microplastics on higher plant *Vicia faba*. *Environmental Pollution*, 250, 831–838. <https://doi.org/10.1016/j.envpol.2019.04.055>
- Kawano, T., Tanaka, S., Kadono, T. & Muto, S. (2004) Salicylic acid glucoside acts as a slow inducer of oxidative burst in tobacco suspension culture. *Zeitschrift für Naturforschung C*, 59, 684–692. <https://doi.org/10.1515/znc-2004-9-1013>
- Koelmans, A.A., Besseling, E. & Shim, W.J. (2015) Nanoplastics in the aquatic environment. Critical review. In: Bergmann, M., Gutow, L. & Klages, M., Eds *Marine Anthropogenic Litter*. Cham: Springer International Publishing. pp. 325–340. [https://doi.org/10.1007/978-3-319-16510-3\\_12](https://doi.org/10.1007/978-3-319-16510-3_12)
- Koevoets, I.T., Venema, J.H., Elzenga, J.T.M. & Testerink, C. (2016) Roots withstanding their environment: exploiting root system architecture responses to abiotic stress to improve crop tolerance. *Frontiers in Plant Science*, 07, 1335. <https://doi.org/10.3389/fpls.2016.01335>
- Kokalj, A.J., Hartmann, N.B., Drobne, D., Potthoff, A. & Kühnel, D. (2021) Quality of nanoplastics and microplastics ecotoxicity studies: refining quality criteria for nanomaterial studies. *Journal of Hazardous Materials*, 415, 125751. <https://doi.org/10.1016/j.jhazmat.2021.125751>
- Kong, X., Zhang, C., Zheng, H., Sun, M., Zhang, F., Zhang, M. et al. (2020) Antagonistic interaction between auxin and SA signaling pathways regulates bacterial infection through lateral root in *Arabidopsis*. *Cell Reports*, 32, 108060. <https://doi.org/10.1016/j.celrep.2020.108060>
- Larue, C., Castillo-Michel, H., Sobanska, S., Cécillon, L., Bureau, S., Barthès, V. et al. (2014) Foliar exposure of the crop *Lactuca sativa* to silver nanoparticles: evidence for internalization and changes in Ag speciation. *Journal of Hazardous Materials*, 264, 98–106. <https://doi.org/10.1016/j.jhazmat.2013.10.053>
- Larue, C., Sarret, G., Castillo-Michel, H. & Pradas del Real, A.E. (2021) A critical review on the impacts of nanoplastics and microplastics on aquatic and terrestrial photosynthetic organisms. *Small*, 17, 2005834. <https://doi.org/10.1002/sml.202005834>
- Li, C., Gao, Y., He, S., Chi, H.-Y., Li, Z.-C., Zhou, X.-X. et al. (2021) Quantification of nanoplastic uptake in cucumber plants by pyrolysis gas chromatography/mass spectrometry. *Environmental Science & Technology Letters*, 8, 633–638.
- Li, L., Luo, Y., Li, R., Zhou, Q., Peijnenburg, W.J.G.M., Yin, N. et al. (2020) Effective uptake of submicrometre plastics by crop plants via a crack-entry mode. *Nature Sustainability*, 3, 929–937. <https://doi.org/10.1038/s41893-020-0567-9>
- Li, L., Luo, Y., Peijnenburg, W.J.G.M., Li, R., Yang, J. & Zhou, Q. (2020) Confocal measurement of microplastics uptake by plants. *MethodsX*, 7, 100750. <https://doi.org/10.1016/j.mex.2019.11.023>
- Li, Z., Li, Q., Li, R., Zhou, J. & Wang, G. (2021) The distribution and impact of polystyrene nanoplastics on cucumber plants. *Environmental Science and Pollution Research*, 28, 16042–16053. <https://doi.org/10.1007/s11356-020-11702-2>
- Lian, J., Liu, W., Meng, L., Wu, J., Chao, L., Zeb, A. et al. (2021) Foliar-applied polystyrene nanoplastics (PSNPs) reduce the growth and nutritional quality of lettuce (*Lactuca sativa* L.). *Environmental Pollution*, 280, 116978. <https://doi.org/10.1016/j.envpol.2021.116978>
- Lian, J., Liu, W., Sun, Y., Men, S., Wu, J., Zeb, A. et al. (2022) Nanotoxicological effects and transcriptome mechanisms of wheat (*Triticum aestivum* L.) under stress of polystyrene nanoplastics. *Journal of Hazardous Materials*, 423, 127241. <https://doi.org/10.1016/j.jhazmat.2021.127241>
- Liu, Y., Guo, R., Zhang, S., Sun, Y. & Wang, F. (2022) Uptake and translocation of nano/microplastics by rice seedlings: evidence from a hydroponic experiment. *Journal of Hazardous Materials*, 421, 126700. <https://doi.org/10.1016/j.jhazmat.2021.126700>

- Liu, Y., Li, J., Parakhonskiy, B.V., Hoogenboom, R., Skirtach, A. & De Neve, S. (2024) Labelling of micro- and nanoplastics for environmental studies: state-of-the-art and future challenges. *Journal of Hazardous Materials*, 462, 132785. <https://doi.org/10.1016/j.jhazmat.2023.132785>
- Luo, Y., Li, L., Feng, Y., Li, R., Yang, J., Peijnenburg, W.J.G.M. et al. (2022) Quantitative tracing of uptake and transport of submicrometre plastics in crop plants using lanthanide chelates as a dual-functional tracer. *Nature Nanotechnology*, 17, 424–431. <https://doi.org/10.1038/s41565-021-01063-3>
- Lwanga, E.H., Beriot, N., Corradini, F., Silva, V., Yang, X., Baartman, J. et al. (2022) Review of microplastic sources, transport pathways and correlations with other soil stressors: a journey from agricultural sites into the environment. *Chemical and Biological Technologies in Agriculture*, 9, 20. <https://doi.org/10.1186/s40538-021-00278-9>
- Maity, S., Guchhait, R., Sarkar, M.B. & Pramanick, K. (2022) Occurrence and distribution of micro/nanoplastics in soils and their phytotoxic effects: A review. *Plant, Cell & Environment*, 45, 1011–1028. <https://doi.org/10.1111/pce.14248>
- Mariano, S., Tacconi, S., Fidaleo, M., Rossi, M. & Dini, L. (2021) Micro and nanoplastics identification: classic methods and innovative detection techniques. *Frontiers in Toxicology*, 3, 636640. <https://doi.org/10.3389/ftox.2021.636640>
- Mattsson, K., Ekvall, M.T., Hansson, L.-A., Linse, S., Malmendal, A. & Cedervall, T. (2015) Altered behavior, physiology, and metabolism in fish exposed to polystyrene nanoparticles. *Environmental Science & Technology*, 49, 553–561. <https://doi.org/10.1021/es5053655>
- Neugart, S., Wiesner-Reinhold, M., Frede, K., Jander, E., Homann, T., Rawel, H.M. et al. (2018) Effect of solid biological waste compost on the metabolite profile of *Brassica rapa ssp. chinensis*. *Frontiers in Plant Science*, 9, 305. <https://doi.org/10.3389/fpls.2018.00305>
- Parween, T. & Jan, S. (2020) Strategies for preventing and controlling pesticide toxicity, in: *Ecophysiology of Pesticides*. Elsevier. pp. 265–304. <https://doi.org/10.1016/B978-0-12-817614-6.00008-1>
- Pérez-Reverón, R., Álvarez-Méndez, S.J., Kropp, R.M., Perdomo-González, A., Hernández-Borges, J. & Díaz-Peña, F.J. (2022) Microplastics in agricultural systems: analytical methodologies and effects on soil quality and crop yield. *Agriculture (London)*, 12, 1162.
- Plastics Europe(2022) Plastics—the facts 2022, *Plastics Europe*. <https://plasticseurope.org/knowledge-hub/plastics-the-facts-2022/>
- Qi, R., Jones, D.L., Li, Z., Liu, Q. & Yan, C. (2020) Behavior of microplastics and plastic film residues in the soil environment: a critical review. *Science of the Total Environment*, 703, 134722. <https://doi.org/10.1016/j.scitotenv.2019.134722>
- Rong, S., Wang, S., Liu, H., Li, Y., Huang, J. & Wang, W. et al. (2024) Evidence for the transportation of aggregated microplastics in the symplast pathway of oilseed rape roots and their impact on plant growth. *Science of the Total Environment*, 912, 169419. <https://doi.org/10.1016/j.scitotenv.2023.169419>
- Rose, P.K., Yadav, S., Kataria, N. & Khoo, K.S. (2023) Microplastics and nanoplastics in the terrestrial food chain: uptake, translocation, trophic transfer, ecotoxicology, and human health risk. *TrAC, Trends in Analytical Chemistry*, 167, 117249. <https://doi.org/10.1016/j.trac.2023.117249>
- Roy, T., Dey, T.K. & Jamal, M. (2023) Microplastic/nanoplastic toxicity in plants: an imminent concern. *Environmental Monitoring and Assessment*, 195, 27. <https://doi.org/10.1007/s10661-022-10654-z>
- Ruan, J., Zhou, Y., Zhou, M., Yan, J., Khurshid, M., Weng, W. et al. (2019) Jasmonic acid signaling pathway in plants. *International Journal of Molecular Sciences*, 20, 2479. <https://doi.org/10.3390/ijms20102479>
- Sahai, H., Bueno, M.J.M., del Mar Gómez-Ramos, M., Fernández-Alba, A.R. & Hernando, M.D. (2024) Quantification of nanoplastic uptake and distribution in the root, stem and leaves of the edible herb *Lepidium sativum*. *Science of the Total Environment*, 912, 168903. <https://doi.org/10.1016/j.scitotenv.2023.168903>
- Schwaferts, C., Niessner, R., Elsner, M. & Ivleva, N.P. (2019) Methods for the analysis of submicrometer- and nanoplastic particles in the environment. *TrAC, Trends in Analytical Chemistry*, 112, 52–65. <https://doi.org/10.1016/j.trac.2018.12.014>
- Shi, Y., Shi, L., Huang, H., Ye, K., Yang, L., Wang, Z. et al. (2024) Analysis of aged microplastics: a review. *Environmental Chemistry Letters*, 22, 1861–1888. <https://doi.org/10.1007/s10311-024-01731-5>
- Spielman-Sun, E., Avellan, A., Bland, G.D., Tappero, R.V., Acerbo, A.S., Unrine, J.M. et al. (2019) Nanoparticle surface charge influences translocation and leaf distribution in vascular plants with contrasting anatomy. *Environmental Science: Nano*, 6, 2508–2519. <https://doi.org/10.1039/C9EN00626E>
- Sun, H., Lei, C., Xu, J. & Li, R. (2021) Foliar uptake and leaf-to-root translocation of nanoplastics with different coating charge in maize plants. *Journal of Hazardous Materials*, 416, 125854. <https://doi.org/10.1016/j.jhazmat.2021.125854>
- Sun, H., Wang, M., Lei, C. & Li, R. (2021) Cell wall: an important medium regulating the aggregation of quantum dots in maize (*Zea mays* L.) seedlings. *Journal of Hazardous Materials*, 403, 123960. <https://doi.org/10.1016/j.jhazmat.2020.123960>
- Sun, H., Wang, M., Wang, J. & Wang, W. (2022) Surface charge affects foliar uptake, transport and physiological effects of functionalized graphene quantum dots in plants. *Science of the Total Environment*, 812, 151506. <https://doi.org/10.1016/j.scitotenv.2021.151506>
- Sun, X.-D., Yuan, X.-Z., Jia, Y., Feng, L.-J., Zhu, F.-P., Dong, S.-S. et al. (2020) Differentially charged nanoplastics demonstrate distinct accumulation in *Arabidopsis thaliana*. *Nature Nanotechnology*, 15, 755–760. <https://doi.org/10.1038/s41565-020-0707-4>
- Tian, J., Xu, Z., Huang, W., Han, D., Dang, B., Xu, J. et al. (2024) Physio-biochemical and transcriptional responses of tobacco plants (*Nicotiana tabacum* L.) to different doses of polystyrene nanoplastics. *Industrial Crops and Products*, 220, 119218. <https://doi.org/10.1016/j.indcrop.2024.119218>
- Tympa, L.-E., Katsara, K., Moschou, P.N., Kenanakis, G. & Papadakis, V.M. (2021) Do microplastics enter our food chain via root vegetables? A Raman based spectroscopic study on *Raphanus sativus*. *Materials*, 14, 2329. <https://doi.org/10.3390/ma14092329>
- UN Environment Programme (2022) Plastic pollution [WWW Document], UNEP—UN Environment Programme. <http://www.unep.org/plastic-pollution>
- Vithanage, M., Ramanayaka, S., Hasinthara, S. & Navaratne, A. (2021) Compost as a carrier for microplastics and plastic-bound toxic metals into agroecosystems. *Current Opinion in Environmental Science & Health*, 24, 100297. <https://doi.org/10.1016/j.coesh.2021.100297>
- Völz, R., Park, J.-Y., Harris, W., Hwang, S. & Lee, Y.-H. (2021) Lyso-phosphatidylethanolamine primes the plant immune system and promotes basal resistance against hemibiotrophic pathogens. *BMC Biotechnology*, 21, 12. <https://doi.org/10.1186/s12896-020-00661-8>
- Wang, H., Kou, X., Pei, Z., Xiao, J.Q., Shan, X. & Xing, B. (2011) Physiological effects of magnetite (Fe<sub>3</sub>O<sub>4</sub>) nanoparticles on perennial ryegrass (*Lolium perenne* L.) and pumpkin (*Cucurbita mixta*) plants. *Nanotoxicology*, 5, 30–42. <https://doi.org/10.3109/17435390.2010.489206>
- Wu, J., Liu, W., Zeb, A., Lian, J., Sun, Y. & Sun, H. (2021) Polystyrene microplastic interaction with *Oryza sativa*: toxicity and metabolic mechanism. *Environmental Science: Nano*, 8, 3699–3710. <https://doi.org/10.1039/D1EN00636C>
- Xiong, T., Dumat, C., Dappe, V., Vezin, H., Schreck, E., Shahid, M. et al. (2017) Copper oxide nanoparticle foliar uptake, phytotoxicity, and consequences for sustainable urban agriculture. *Environmental Science & Technology*, 51, 5242–5251. <https://doi.org/10.1021/acs.est.6b05546>
- Ye, Q., Wu, Y., Liu, W., Ma, X., He, D., Wang, Y. et al. (2024) Identification and quantification of nanoplastics in different crops using pyrolysis gas chromatography-mass spectrometry. *Chemosphere*, 354, 141689. <https://doi.org/10.1016/j.chemosphere.2024.141689>

- Yu, H., Zhang, Y., Tan, W. & Zhang, Z. (2022) Microplastics as an emerging environmental pollutant in agricultural soils: effects on ecosystems and human health. *Frontiers in Environmental Science*, 10, 855292. <https://doi.org/10.3389/fenvs.2022.855292>
- Yu, Y., Griffin-LaHue, D.E., Miles, C.A., Hayes, D.G. & Flury, M. (2021) Are micro- and nanoplastics from soil-biodegradable plastic mulches an environmental concern? *Journal of Hazardous Material*, 4, 100024. <https://doi.org/10.1016/j.hazadv.2021.100024>
- Zhou, C.-Q., Lu, C.-H., Mai, L., Bao, L.-J., Liu, L.-Y. & Zeng, E.Y. (2021) Response of rice (*Oryza sativa* L.) roots to nanoplastic treatment at seedling stage. *Journal of Hazardous Materials*, 401, 123412. <https://doi.org/10.1016/j.jhazmat.2020.123412>

## SUPPORTING INFORMATION

Additional supporting information can be found online in the Supporting Information section at the end of this article.

**How to cite this article:** Zytowski, E., Mollavali, M. & Baldermann, S. (2025) Uptake and translocation of nanoplastics in mono and dicot vegetables. *Plant, Cell & Environment*, 48, 134–148. <https://doi.org/10.1111/pce.15115>